Electronic Supplementary Information

Reductive conversion of Cr(VI) to Cr(III) over bimetallic CuNi nanocrystals at room temperature

Biraj Jyoti Borah, Himadri Saikia and Pankaj Bharali*

Department of Chemical Sciences, Tezpur University, Napaam, Tezpur 784 028, India

Submitted to New Journal of Chemistry

Synthesis of Cu, Ni and CuNi bimetallic nanocrystals:

All the reagents were analytical grade and used without further purification. In a typical procedure, to prepare CuNi, 50 ml aqueous solution of 0.426 g (100 mM) $CuCl_2{\cdot}2H_2O$ (Merck, India) and 0.594 g (100 mM) $NiCl_2{\cdot}6H_2O$ (Merck, India) is added to 50 ml NaOH (Merck, India) solution (0.8 gm, 0.4 M) at room temperature under constant stirring. After stirring about 15 min, 3.5 ml of 85 % hydrazine hydrate (Merck, India) was added dropwise to the mixture and stirred vigorously. After about 20 min the solution was transferred into a Teflon cup (250 ml capacity) in a stainless steel autoclave. The autoclave was sealed and kept in an oven and maintained at 120 °C for 6 h. The autoclave was allowed to cool naturally (2.5 h); a black fluffy solid product was deposited on the bottom of the Teflon cup which indicates the formation of CuNi bimetallic nanocrystals. The final product was washed several times with distilled water and then 50% C_2H_5OH solution to remove the un-reacted NaOH and Cl^-, and finally collected by centrifugation. The product was dried in a vacuum oven at 55 °C for 12 h. Identical procedure was employed to prepare various compositions of CuNi bimetallic as well as monometallic Cu and Ni nanocrystals (Table S1).

Table S1: The amount of precursor metal salts employed for the syntheses of various CuNi bimetallic nanocrystals of different composition as well as monometallic Cu and Ni nanocrystals

Composition	Amount of $CuCl_2{\cdot}2H_2O$	Amount of $NiCl_2{\cdot}6H_2O$
Cu_2Ni_3	0.3408 g (80 mM)	0.7131 g (120 mM)
CuNi	0.426 g (100 mM)	0.594 g (100 mM)
Cu_3Ni_2	0.5112 g (150 mM)	0.4754 g (80 mM)
Cu	0.852 g (200 mM)	–
Ni	–	1.19 g (200 mM)

Characterization of nanocrystals:

The powder XRD patterns were recorded on a Rigaku Multiflex instrument using nickel-filtered CuKα (0.15418 nm) radiation source and a scintillation counter detector. The intensity data were collected over a 2θ range of 5−90°. SEM analyses were carried out with "JEOL, JSM Model 6390 LV" scanning electron microscope, operating at an accelerating voltage of 15 kV. EDX spectra as well as element mapping analyses were also performed in the same instrument attached to the scanning electron microscope. The TEM and HRTEM investigations were carried on a JEM-2010 (JEOL) instrument equipped with a slow-scan CCD camera and at an accelerating voltage of 200 kV. The BET surface areas were determined by N_2 adsorption using a Quantachrome Instruments (Model: NOVA 1000e). UV-visible spectra were taken on a UV-visible spectrophotometer, Shimadzu Corporation (UV-2550).

Reductive conversion of Cr(VI) to Cr(III):

The catalytic reduction of Cr(VI) was carried out in a glass reactor with constant stirring (650-660 rpm) in the presence of various compositions of CuNi bimetallic as well as monometallic Cu and Ni catalysts using HCOOH as reducing agent. In a typical procedure, to 20 ml (0.2 mM) aqueous $Cr_2O_7^{2-}$ (Cr(VI)) solution purged with inert N_2 (to remove the dissolved oxygen) 1 ml HCOOH (100%, Merck, India) was added. $K_2Cr_2O_7$ (Merck, India) was chosen as representative of Cr(VI) source. $Cr_2O_7^{2-}$ exhibits strong absorption centred at 348 nm of the UV-visible spectrum due to the ligand (O^{2-}) to metal (Cr(VI)) charge-transfer transition. An amount of 4 mg of catalysts are employed to investigate the activity studies. The progress of the catalytic reaction was monitored using UV-visible absorption spectroscopy in the wavelength range of 250–550 nm at room temperature (25 °C). The characteristic peak at 348 nm decreases with time confirming the quick reduction of Cr(VI). A change in the color of the reaction solution was also observed from yellow to colorless

with increasing reaction time signifying the reduction of Cr(VI). The presence of Cr(III) was further established by excess addition of NaOH solution, the colorless solution turns green color which characterizes the presence of Cr(III) due to the formation of hexahydroxochromate(III). The UV-visible absorption spectra were also measured in the presence of only HCOOH and only catalysts to demarcate the simultaneous necessity of both HCOOH as well as catalysts for reductive conversion of Cr(VI). The influence of the catalysts' amount and concentration of $Cr_2O_7^{2-}$ (Cr(VI)) on the catalytic activity were also investigated. To test the durability of the CuNi nanocrystals, four successive cycles of catalytic reduction were carried out employing 4 mg of catalyst. In the successive cycles, the catalyst was collected by centrifugation from the previous solution and washed 3 times with distilled water. Further the collected catalyst was applied against the fresh $Cr_2O_7^{2-}$ (Cr(VI)) solution and HCOOH of similar quantity as described previously.

Fig. S1 UV-visible spectra of the reaction solutions for the reductive conversion of Cr(VI) to Cr(III) in the presence of (a) only HCOOH, (b) only Cu_3Ni_2 nanocrystal and (c) the plot of A_t/A_0 versus reaction time derived from the UV-visible data. Reaction condition: HCOOH = 1 ml, $[Cr_2O_7^{2-}]$ = 0.2 mM and catalyst amount = 4 mg.

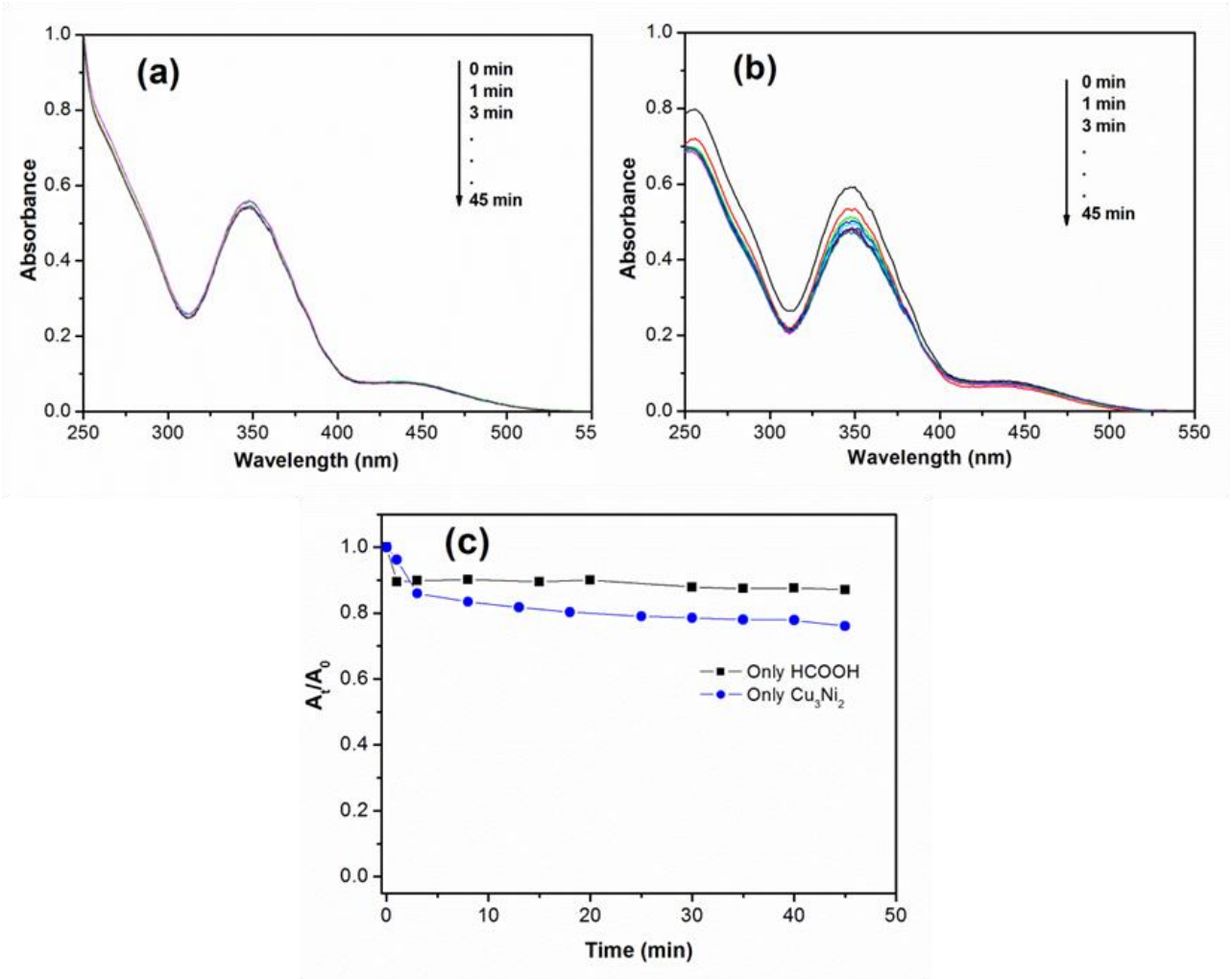

Fig. S2 Plot of Cr(VI) conversion versus reaction time as monitored using UV-visible spectroscopy over different catalysts in the presence of HCOOH at room temperature. Reaction condition: HCOOH = 1 ml, $[Cr_2O_7^{2-}]$ = 0.2 mM and catalyst amount = 4 mg.

Conversion of Cr(VI) was calculated by using the relation -

$$\% \text{ Conversion of Cr(VI)} = (1 - A_t/A_0) \times 100$$

A_t represents absorbance of the 348 nm peak of the UV-visible spectrum at different time interval during catalytic reduction whereas A_0 is the initial absorbance of the 348 nm peak before addition of catalysts.

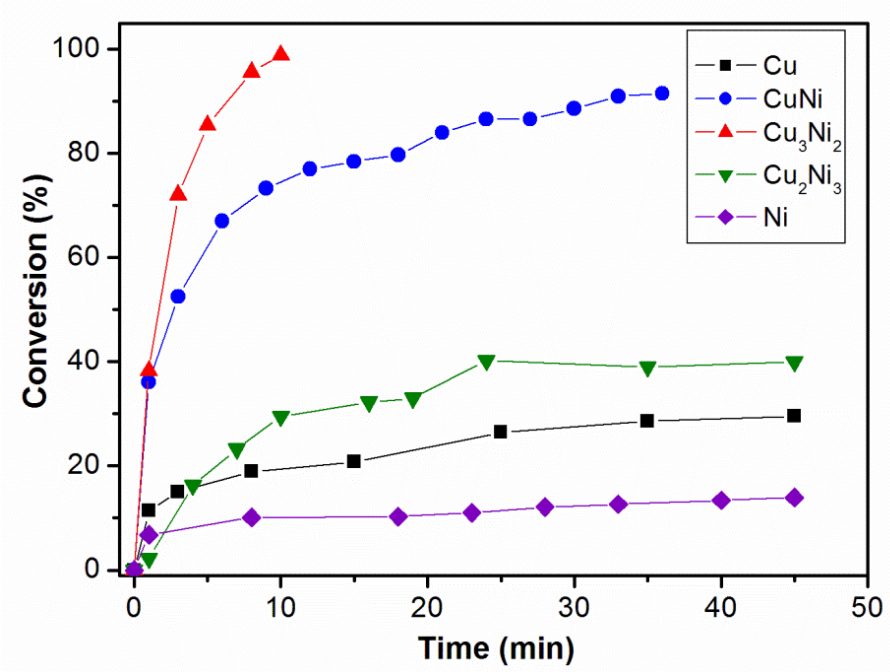

Fig. S3 UV-visible spectra of the reaction solutions for the reductive conversion of Cr(VI) to Cr(III) using different dose of Cu_3Ni_2 nanocatalyst; (a) 1 mg, (b) 2 mg, (c) 4 mg, (d) 6 mg and (e) the plot of A_t/A_0 versus reaction time derived from the UV-visible data. Reaction condition: HCOOH = 1 ml, $[Cr_2O_7^{2-}]$ = 0.2 mM.

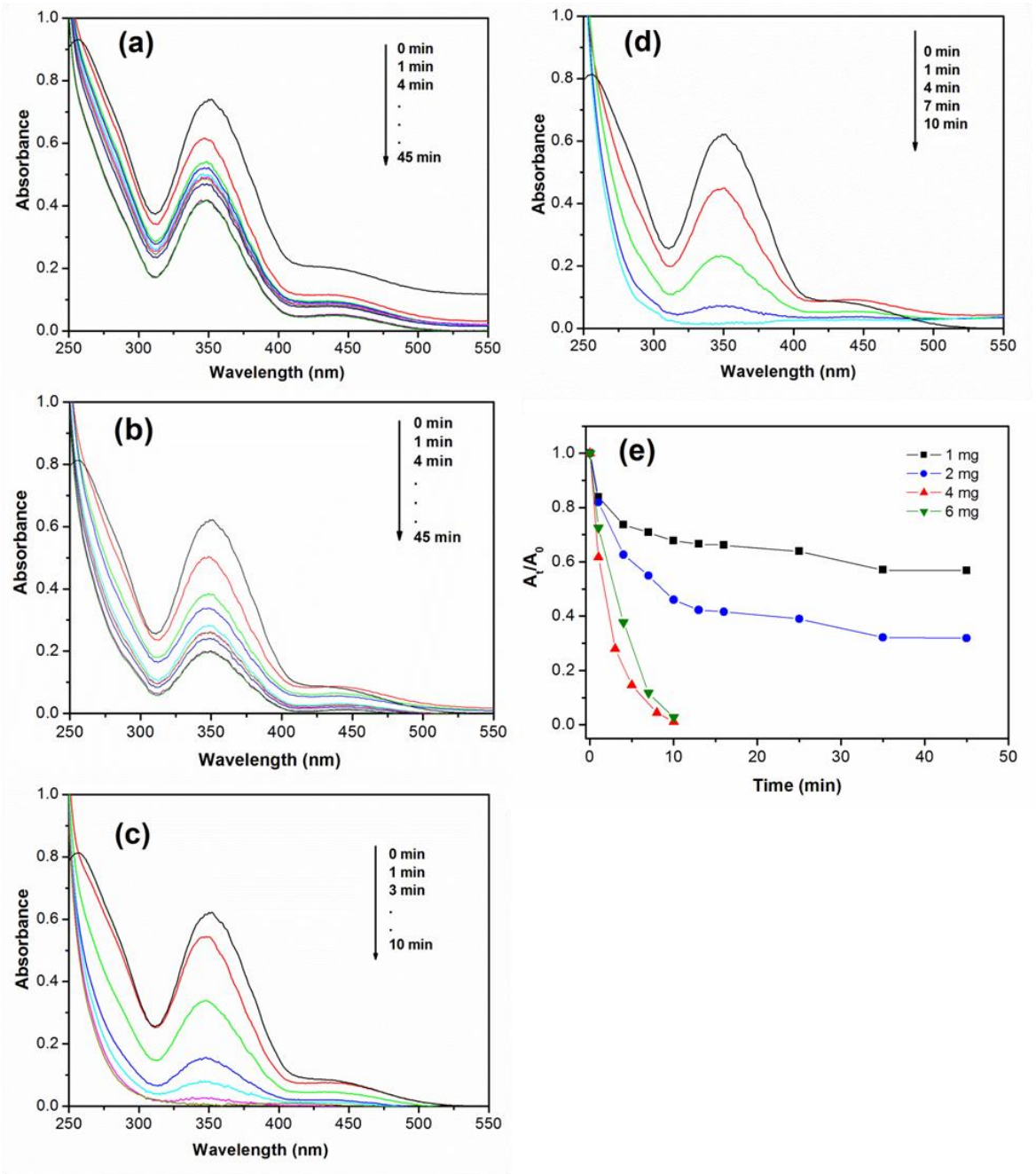

Fig. S4 UV-visible spectra of the reaction solutions for the reductive conversion of Cr(VI) to Cr(III) using different concentration of $Cr_2O_7^{2-}$, i.e. Cr(VI); (a) 0.1 mM, (b) 0.2 mM, (c) 0.3 mM and (d) the plot of A_t/A_0 versus reaction time derived from the UV-visible data. Reaction condition: HCOOH = 1 ml, catalyst amount = 4 mg.

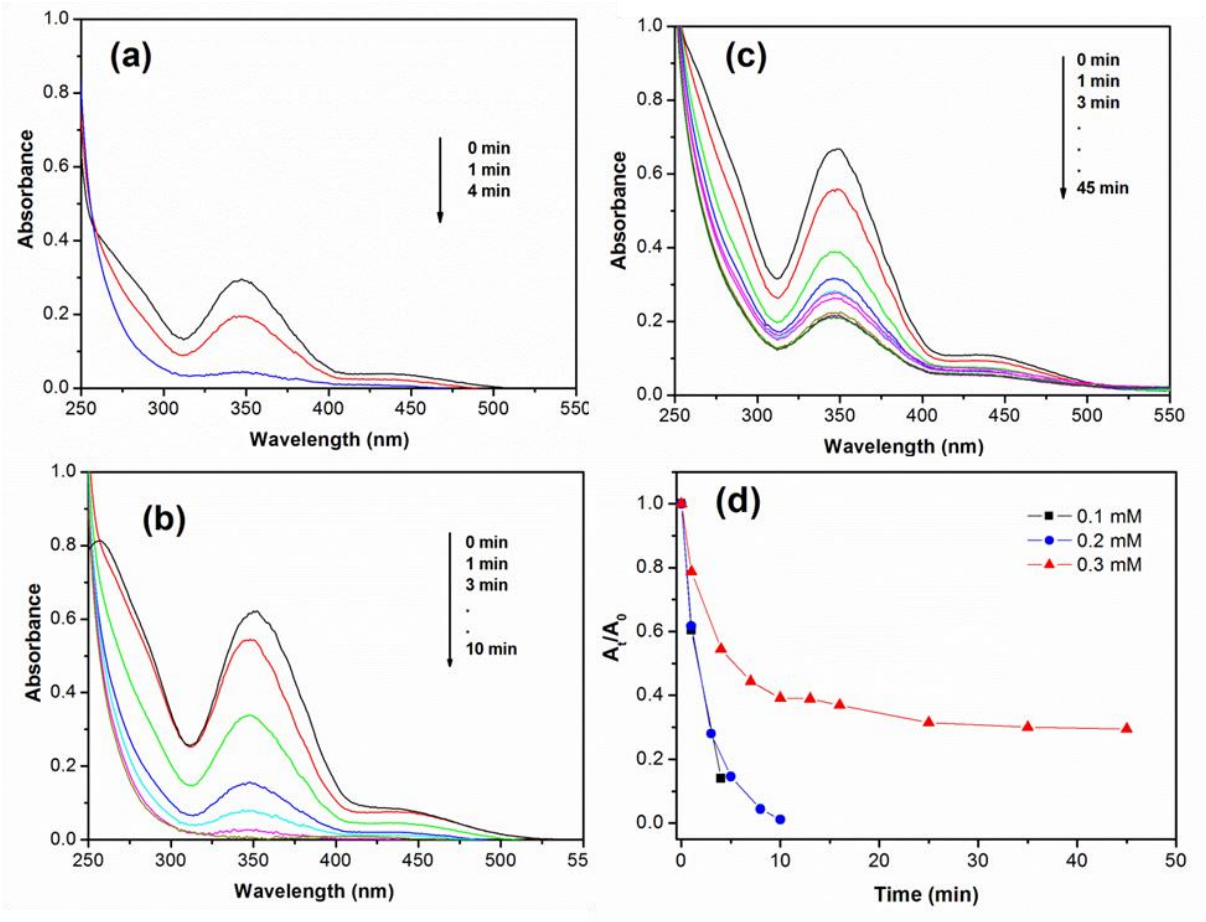

Fig. S5 Conversion against number of cycles of Cr(VI) reduction reaction over Cu_3Ni_2 nanocatalyst for four successive cycles.

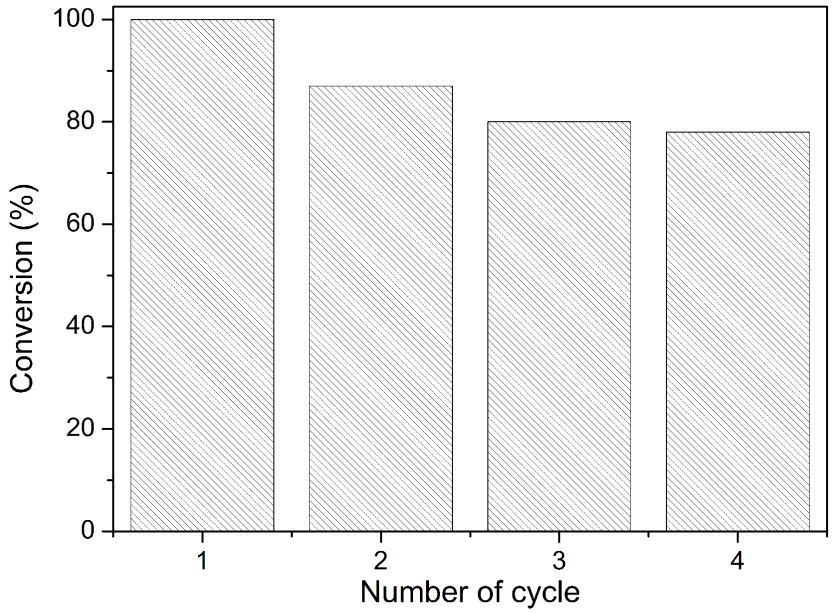

Fig. S6 Transmission electron micrograph of Cu_3Ni_2 nanocrystals after 4th reaction cycle.

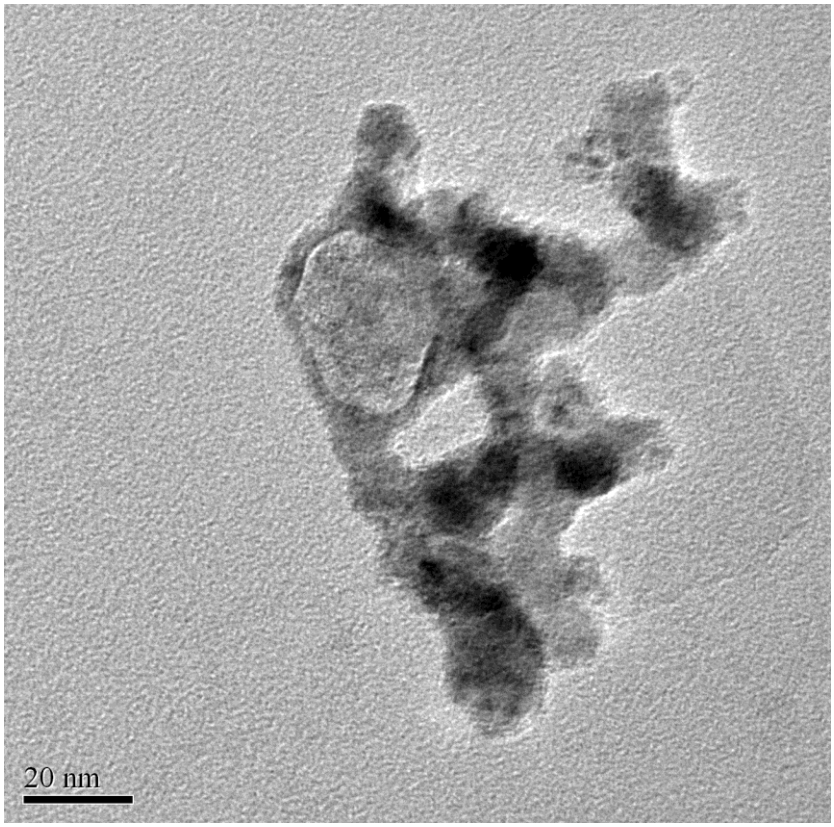

Fig. S7 Scanning electron micrograph of Cu_3Ni_2 nanocatalyst.

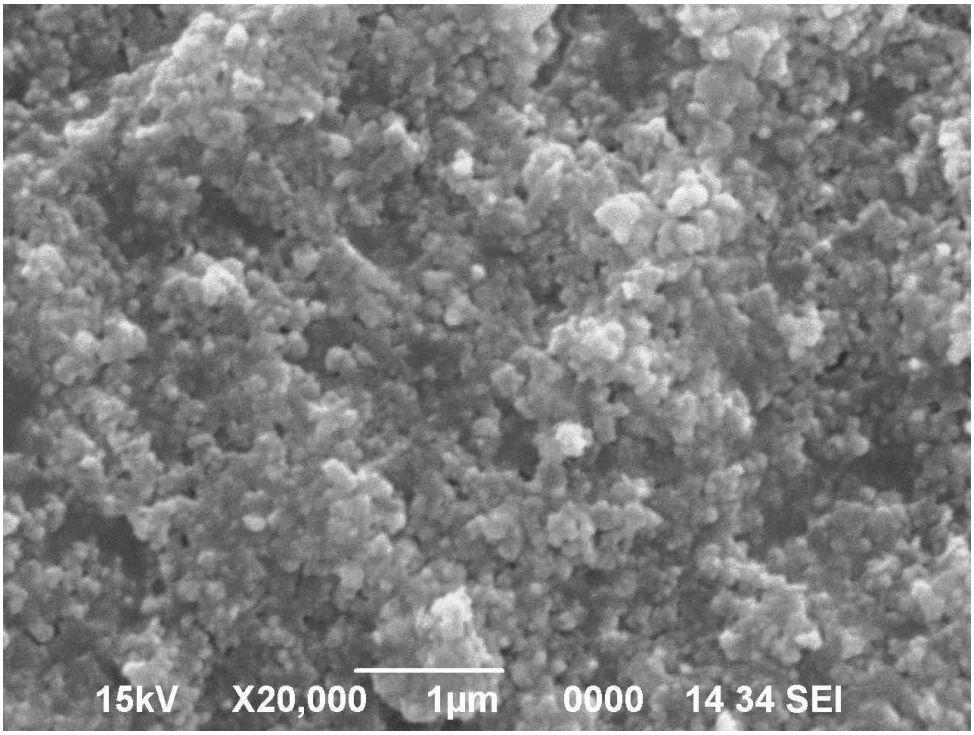

Fig. S8 Energy-dispersive X-ray analysis (EDX) pattern of Cu_3Ni_2 nanocatalyst.

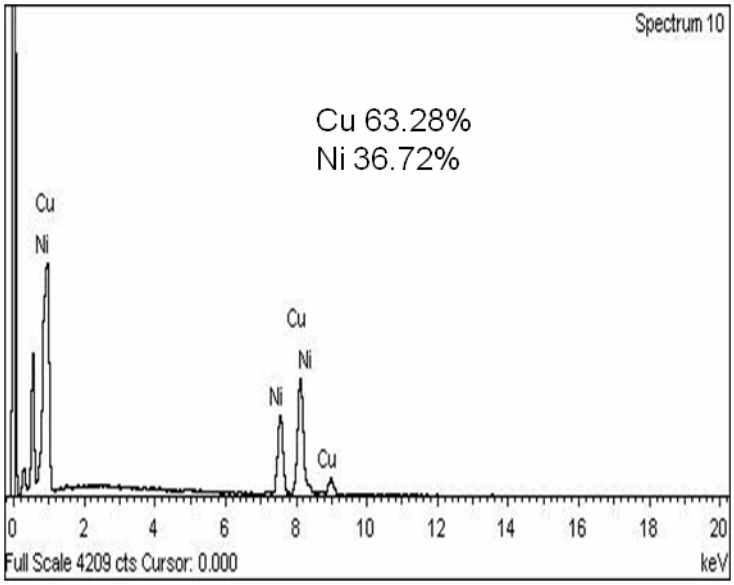

Fig. S9 Nanocrystals size distribution histogram of Cu_3Ni_2 nanocatalyst.

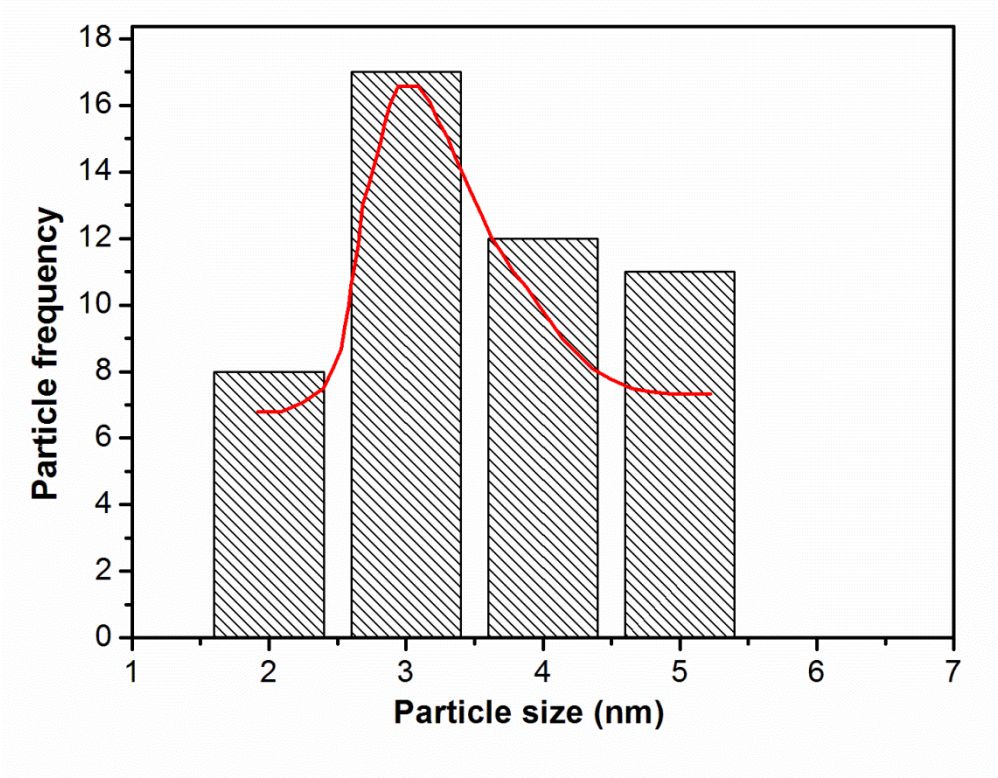

Figure S10: Nitrogen adsorption-desorption isotherm of Cu_3Ni_2 nanocatalyst.

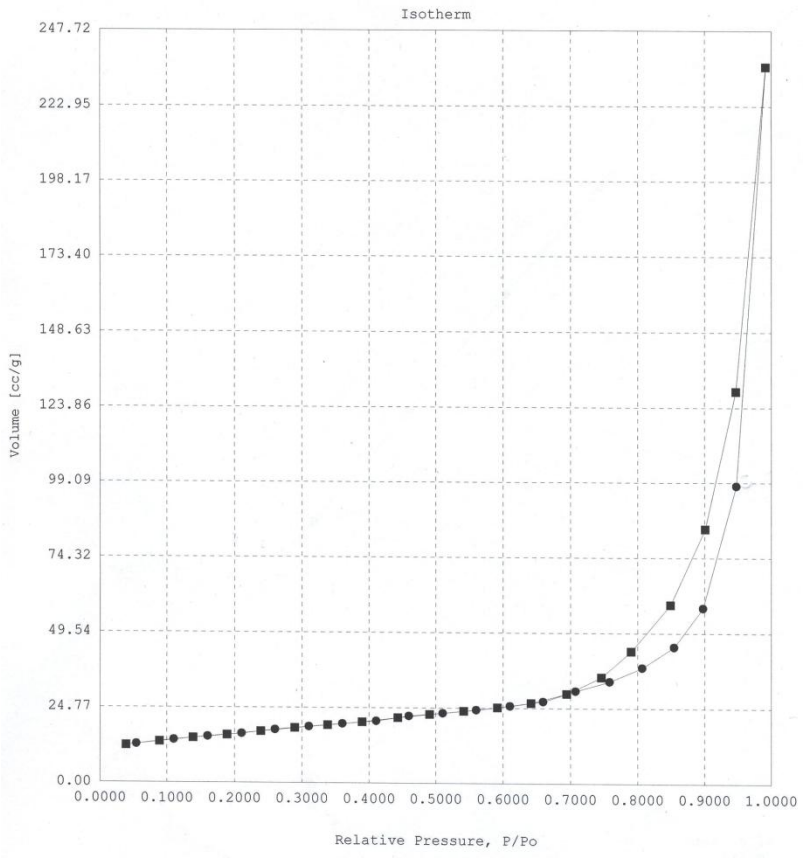

Figure S11: UV-visible spectra of Cu, Ni and Cu_3Ni_2 nanocrystals before and Cu_3Ni_2 after reaction as well as $CuCl_2$ and $NiCl_2$.